Deformation Mechanisms in Constrained Monotonic and Cyclic Compressive Loading of Al Foam

M. MUKHERJEE,
F. GARCIA-MORENO, J. BANHART

Hahn-Meitner-Institute Berlin
Glienicker Strasse 100, 14109 Berlin, Germany

Technical University Berlin
Hardenberg Strasse 36, 10623 Berlin, Germany

M. KOLLURI,
U. RAMAMURTY

Department of Materials Engineering
Indian Institute of Science
Bangalore-560012, India

ABSTRACT

It was reported recently that closed cell Al foams exhibit strain hardening when subjected to monotonic or cyclic loading with lateral constraint. In the present study compressive and fatigue testing was carried out on some Alporas foams with lateral constraint. The deformation mechanisms responsible for this behaviour were examined in this study, by employing non-destructive X-ray tomography on load-interrupted specimens. Foam deformation mechanisms with constraint, studied from the tomograms, were compared with the literature data on foam deformation mechanisms without any constraint. It was found that the deformation mechanisms are similar in both cases.

INTRODUCTION

Metal foams, having unique mechanical properties [1,2], are finding importance in many structural applications [1-4] where they are subjected to compressive or cyclic loading. In many of these applications, especially when the foam is used to fill parts, deformation of the foam occurs under constrained stress conditions. Hence it is necessary to study the deformation behaviour with constraint.

The vast amount of literature on mechanical properties of metal foams focuses on mechanical testing of metal foams without any constraint. In some studies, deformation was carried out on foam filled tubes [5-9]. The strength of the foam filled tubes is higher than the sum of the strength of the two sub-elements (foam and tube). The outer skin of the foam also results in a higher strength of the foam compared to that without any outer skin [9,10]. In all these studies – with the presence of constraint – foam deformation takes place along with the deformation of the constraint. Therefore the effect of constraint separately on the strength of the foam is not clear from these studies. Recently Kolluri et al. [11]

reported the effect of lateral constraint on the mechanical properties of a closed cell Al foam where the foam deformation takes place without any deformation of the constraint. Their experimental results on quasi-static compression indicate that the constraint induces a positive slope to the stress-strain curve in the plastic regime that is not seen without constraint. The strain hardening rate ($d\sigma/d\varepsilon$, where σ is the stress and ε is the strain) with constraint is much higher, 2.59 MPa, compared to the same without constraint, 0.9 MPa. Karthikeyan et al. [12] suggested that multi-axial state of stress and frictional resistance between the deforming foam and the rigid constraint walls are the two sources responsible for the observed hardening. The observed hardening has important practical consequences. For example, Kolluri et al. [13] show that there are marked differences in N_c, the critical number of cycles when strain rises rapidly indicating the onset of stage III of a S-N curve. The stage III initiates relatively earlier in the unconstrained samples followed by a rapid rise in strain level. In contrast, in constrained samples stage III is not a continuous process, but is intervened by periodic slow strain accumulation.

In the present paper, the deformation mechanisms both for monotonic and cyclic compressive loading on samples with lateral constraint were studied with the help of X-ray tomography. The deformation mechanisms were compared with the data available in the literature for similar types of loading but without any constraint.

EXPERIMENTAL

Closed cell aluminium foam, commercial name "Alporas", samples of ~50x50 mm^2 cross section and ~100 mm height were prepared by electro discharge machining. A total of 4 samples were used for testing - samples 1 and 2 for quasi-static compression and samples 3 and 4 for compression-compression fatigue tests. All the samples have similar relative densities (ρ^*) of ~0.09. A die-steel sleeve with a slightly larger inner cross-section than that of

the samples and 118 mm depth was used as constraint during testing. After placing the samples in the sleeve, a solid aluminium block of 50x50 mm^2 cross section was placed on top of the sample. Quasi-static compression and compression-compression fatigue tests were performed in a servo-hydraulic universal testing machine. Quasi-static tests were conducted at a crosshead displacement rate of 0.1 mm/s. Fatigue tests were carried out at a frequency of 10Hz and with a minimum (σ_{min}) to the maximum (σ_{max}) compressive stress ratio of 0.1. Plastic strength (σ_p) of the samples, in MPa, was calculated from ρ^* data by using the equation given by [11]

$$\sigma_p = 60.92 \times \left(\rho^*\right)^{1.5} \qquad (1)$$

The maximum load for the fatigue tests was chosen such that the $\sigma_{max}/\sigma_p = 0.9$. Each test was interrupted at a given amount of strain and X-ray tomography was conducted, after which straining was continued. All the tomograms shown in this paper are binarised boolean images. The strain shown in the tomograms corresponds to the accumulated strain up to that point and does not include the elastic strain because the tomograms were acquired after unloading the sample.

RESULTS AND DISCUSSION

Quasi-static compression

The tomograms in Figure 1 show the vertical section near the central axis of an Alporas foam quasi-statically compressed to various plastic strains. Loading is applied in the vertical direction, shown by an arrow at the top of the foam. The foam is largely homogeneous except for the big pore at the bottom of the foam, Figure 1(a). The corresponding deformed section, Figure 1(b), shows that most of the strain is localized around this big pore, shown by the crush band "1" marked with broken lines. The crush band "1" has a thickness of about 4 to 5 cell diameters. The cells of another band "2" started to buckle in Figure 1(b) and further deformed and formed a collapsed band in Figure 1(c). This band "2" is 3 to 4 cell diameters large. Another crush band "3" of one cell dimension is seen to intersect "2" in Figure 1(c).

Meso-inhomogeneity caused by the presence of the big pore – reflected by the density variation along the height of the foam – results in a higher strain at the bottom of the sample. The big pore reduces local density which in turn reduces the strength of the material. This is in agreement with the results reported by Gradinger et al. [14] who tested foams without any constraint, with similar densities but with different meso-inhomogeneities and found that samples with higher meso-inhomogeneity had lower strength. Sample 2, despite of having a similar density as sample 1, is meso-scopically more homogeneous compared to sample 1, see Figure 2(a). As a result, σ_p is considerably higher for sample 2 (~2.12 MPa) than for sample 1 (~1.66 MPa).

The yz and xz section of sample 2 are shown in Figure 2(a) and (c), respectively. The corresponding deformed

sections, strain level of 25.3%, are shown in Figure 2(b) and (d), respectively. The collapsed bands are shown by pair of broken lines. Although care was taken to make the top and bottom faces of the foam parallel to each other, slight deviation could result in a horizontal band at the top of the foam, such as band nos. 1 and 5. All the collapsed bands sweep the entire foam cross section. They are at an angle with the horizontal axes (x or y). It can be seen that all the collapsed bands are not oriented the same way. Band nos. 2, 3 and 4 in Figure 2(b) make an angle ~15°
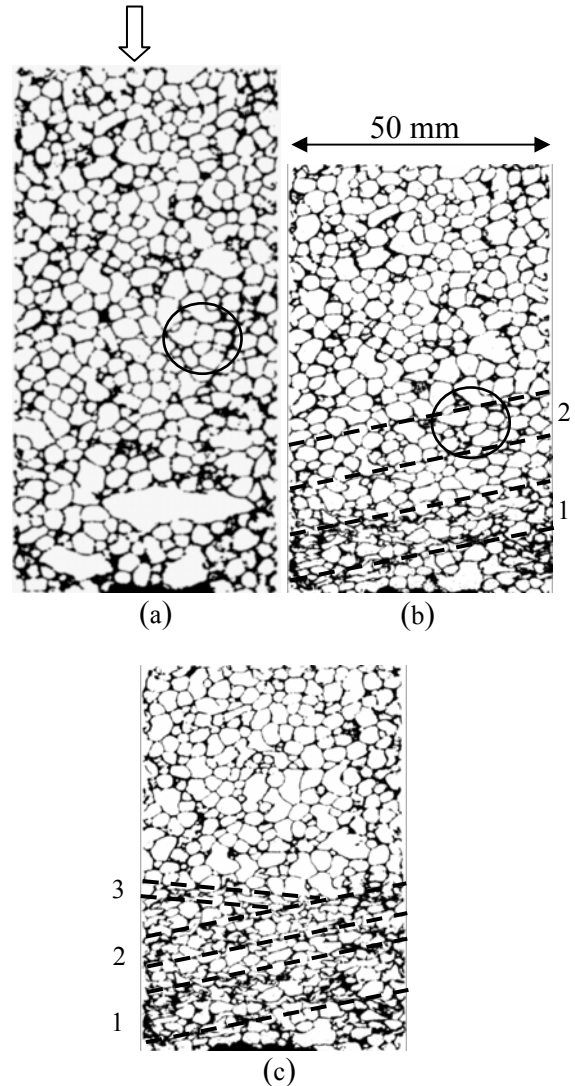

(a)   (b)

(c)

Figure 1. Binarised images of the vertical section of sample 1 that was quasi-statically compressed with lateral constraint, (a) 0%, (b) 17.1% and (c) 25.4% strain. This vertical section is close to the centre of the foam. The arrow in (a) indicate the direction of applied load. It is seen in figure (b) that the biggest pore in the lower part of the foam leads a highest amount of strain localization.

with the horizontal axis, whereas, band no. 6 in Figure 2(d) makes an angle ~13°. Band nos. 8 and 9 have opposite slope and are at an angle ~11°. Band no. 7 is a combination of two intersecting bands. It is similar to band no. 3 in
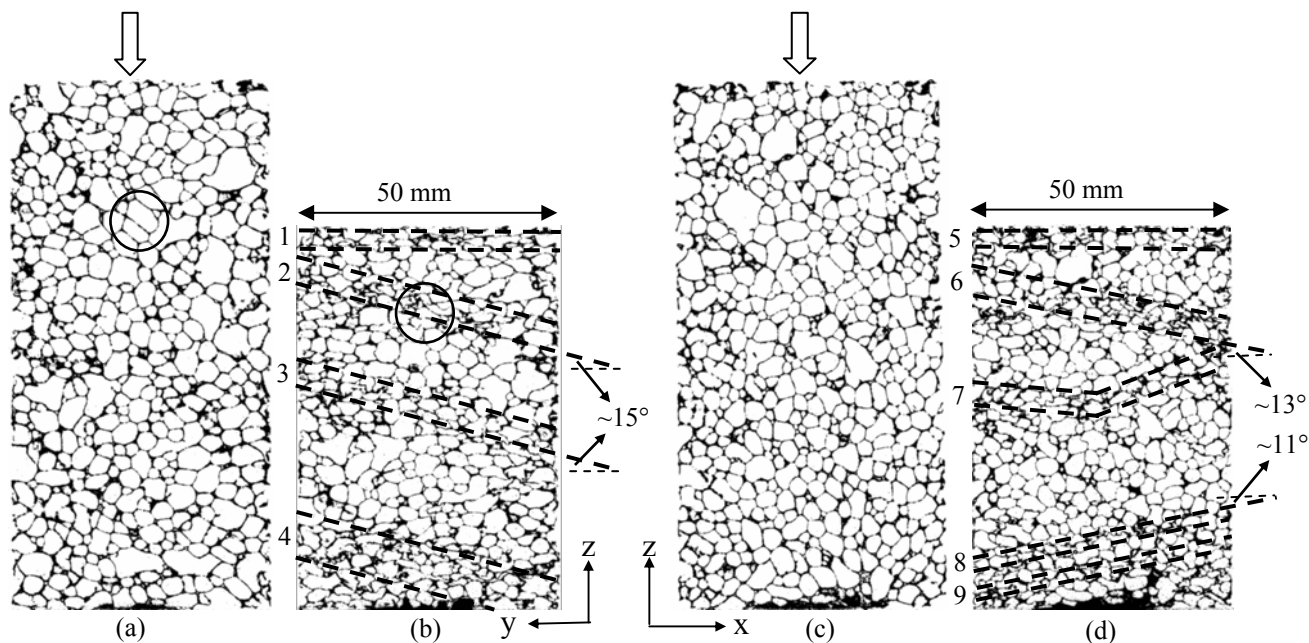
Figure 2. Two perpendicular vertical sections, intersecting near the central axis of the foam, of a quasi-statically compressed with lateral constraint foam (sample 2) are shown. (a) and (b) are the yz and xz section respectively. The arrows in (a) and (c) indicate the loading direction. The corresponding deformed sections after a strain of 25.3% are shown in (b) and (d) respectively. z is the loading direction. Different crush bands are marked by numbers.

Figure 1(c). Band no. 2 in Figure 1(b) has an angle of ~12° with the horizontal axis. Bastawros et al. [15] have tested foams in compression without constraint and have reported that the collapsed bands are at an angle ~20°, but in some instances reach 40°. The angles observed in the present work are lower, within a range of ~11° - 15°. The angle reported in quasi-static compression on a similar foam with constraint is ~15° [11]. It was also reported in Ref 15 that the deformation bands have widths of one cell diameter as compared to the multi-cell band width observed in the present case. Here it should be noted that the tomograms of sample 1 and 2 were acquired above 4% strain. Therefore nothing can be said about the width of a band at a very low strain. However, it can be seen in band no. 2 in Figure 1(b) that buckling started at the same time within a width of 3 cell diameters. Later this formed a collapsed band with 3 cell diameters, see Figure 1(c). Band nos. 8 and 9 in Figure 2(d) have a width of one cell diameter. It can be concluded that the deformation bands are wider than one cell diameter.

Compression-compression fatigue

Figure 3 shows a vertical section of sample 3 which was cyclically tested in compression-compression with lateral constraint, (a) 0% and (b) 13.7% strain. The tomograms of the intermediate strain levels are not shown here. It was observed that a single band forms which then broadens. The same observation was reported by Harte et al. based on their compression-compression fatigue experiments on relatively homogeneous Alporas foams without any constraint [16]. Figure 3(a) reveals that the foam used here also has a homogeneous structure. The angle of the crush band observed by them was ~20° at low strain, later it became constant at a level of ~25° at higher strain. The crush band shown in Figure 3(b) makes an angle ~15° with horizontal.

So far it is seen that there are some differences in orientation and thickness of collapsed bands, between constrained and unconstrained deformation of metal foam both in quasi-static compression and compression-compression fatigue. However, basic macro-mechanisms – progression of deformation by collective cell band collapse, separation of collapsed band by less deformed part – are the same for both constrained and unconstrained deformations. A close look at the tomograms will reveal that the micro-mechanisms which were not discussed here in details are also similar as one would expect in case of unconstrained deformation. For example, the circle-marked regions in Figure 2(a) and (b) show that cell wall deformation is a combination of distortion and shear. The circle-marked regions in Figure 1(a) and (b) show that deformation is only due to distortion. These micro-mechanisms are the same as the ones reported by Bastawros et al. [15]. Formation of cracks in compression-compression fatigue were observed by Kolluri et al. [13] in case of constrained deformation and by Sugimura et al. [17] in case of unconstrained deformation. Hence, the micro-mechanisms are also the same both for constrained and unconstrained deformation. The only difference is that in constrained deformation there is no shearing displacement – which is an obvious effect of constraint –
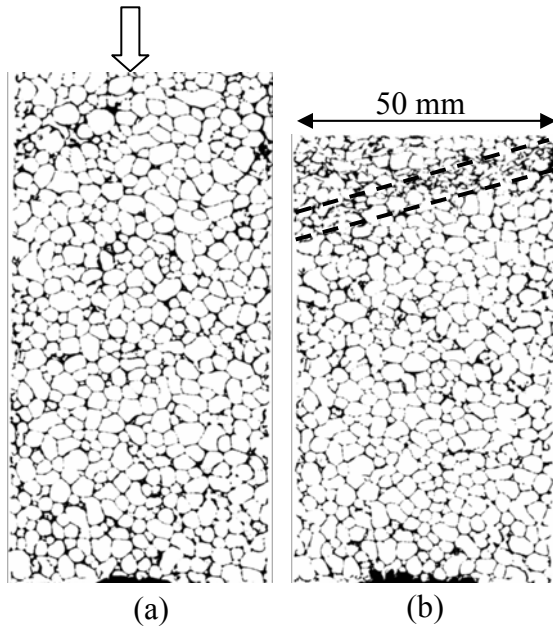
Figure 3. (a) Vertical section (yz) near the central axis of an Alporas foam tested in compression-compression fatigue with lateral constraint. (b) The same section is shown after a strain of 13.7%. The arrow in (a) indicates the direction of loading. Deformation is localised at one crush band. Rest of the foam shows very little strain.

as one would expect in case of constrained deformation.

CONCLUSIONS

Deformation mechanisms of foams tested both in quasi-statically compression and cyclic compression-compression with lateral constraints were investigated by X-ray tomography. The observations were compared with the data available in the literature for unconstrained tested foams. It was found that although there are some differences, the fundamental deformation mechanisms are similar for constrained and unconstrained testing conditions.

REFERENCES

1. Banhart, J. 2001. "Manufacture, Characterisation and Application of Cellular Metals and Metal Foams," *Prog. Mat. Sci.*, 46: 559-632.
2. Ashby, M. F., A. G. Evans, N. A. Fleck, L. J. Gibson, J. W. Hutchinson, and H. N. G. Wadley. 2000. "Metal Foams: A Design Guide," Boston: Butterworth-Heinemann.
3. Yu, C.-J., H. H. Eifert, J. Banhart, and J. Baumeister. 1998. "Metal Foaming by a Powder Metallurgy Method: Production, Properties and Applications," *Mat. Res. Innovat.*, 2: 181-188.
4. Banhart, J. 2005. "Aluminium Foams for Lighter Vehicles," *Int. J. Vehicle Design*, 37: 114-125.
5. Hanssen, A. G., M. Langseth, and O. S. Hopperstad. 1999. "Static Crushing of Square Aluminium Extrusions with Aluminium Foam Filler," *Int. J. Mech. Sci*, 41: 967-993.
6. Hanssen, A. G., M. Langseth, and O. S. Hopperstad. 2000. "Static and Dynamic Crushing of Square Aluminium Extrusions with Aluminium Foam Filler," *Int. J. Impact Eng.*, 24: 347-383.
7. Hanssen, A. G., M. Langseth, and O. S. Hopperstad. 2000. "Static and Dynamic Crushing of Circular Aluminium Extrusions with Aluminium Foam Filler," *Int. J. Impact Eng.*, 24: 475-507.
8. Hanssen, A. G., M. Langseth, and O. S. Hopperstad. 2001. "Optimum Design for Energy Absorption of Square Aluminium Columns with Aluminium Foam Filler," *Int. J. Mech. Sci.*, 43: 153-176.
9. Peroni, L., M. Avalle, and M. Peroni. "The Mechanical Behaviour of Aluminium Foam Structures in Different Loading Conditions," *Int. J. Impact Eng.*, doi: 10.1016/j.ijimpeng.2007.02.007.
10. Banhart, J. and J. Baumeister. 1998. "Deformation Characteristics of Metal Foams," *J. Mat. Sci.*, 33: 1413-1440.
11. Kolluri, M., S. Karthikeyan, and U. Ramamurty. 2007. "Effect of Lateral Constraint on the Mechanical Properties of a Closed-cell Al Foam: I. Experiments," *Met. Mat. Trans. A*, 38A: 2006-2013.
12. Karthikeyan, S., M. Kolluri, and U. Ramamurty. 2007. "Effect of Lateral Constraint on the Mechanical Properties of a Closed-cell Al Foam: Part II. Strain-Hardening Models," *Met. Mat. Trans. A*, 38A: 2014-2023.
13. Kolluri, M., M. Mukherjee, F. Garcia-Moreno, J. Banhart, and U. Ramamurty. "Constrained Fatigue in a Closed Cell Aluminium Foam," to be published.
14. Gradinger, R., and F. G. Rammerstorfer. 1999. "On the Influence of Meso-inhomogeneities on the Crush Worthiness of Metal Foams," *Acta Mater.*, 47(1): 143-148.
15. Bastawros, A.-F., H. Bart-Smith, and A. G. Evans. 2000. "Experimental Analysis of Deformation Mechanisms in a Closed-cell Aluminium Alloy Foam," *J. Mech. Phy. Sol.*, 48: 301-322.
16. Harte, A.-M., N. A. Felck, and M. F. Ashby. 1999. "Fatigue Failure of an Open Cell and a Closed Cell Aluminium Alloy Foam," *Acta Mater.*, 47(8): 2511-2524.
17. Sugimura, Y., A. Rabiei, A. G. Evans, A. M. Harte, and N. A. Felck. 1999. "Compression Fatigue of a Cellular Al Alloy," *Mat. Sci. Engg.*, A269: 38-48.